COSMIC Status and Prospects for COSMIC-II

Ying-Hwa Kuo[1], Hui Liu[2], Zaizhong Ma[2], sergey Sokolovskiy[1], Peng Guo[1], Richard A. Anthes[1], Nick Yen[3], and Jiun-Jih Miau[3]

[1]University Corporation for Atmospheric Research, Boulder, Colorado, USA
[2]National Center for Atmospheric Research, Boulder, Colorado, USA
[3]National Space Organization, Hsin-Chu, Taiwan

Abstract

The launch of the joint Taiwan-U.S. COSMIC/FORMOSAT-3 (Constellation Observing System for Meteorology, Ionosphere, and Climate, and Formosa Satellite mission #3; hereafter COSMIC) mission in April 2006 marks the beginning of a new era for GPS (Global Positioning System) atmospheric remote sensing. As of October 2008, COSMIC had taken 1.4 million neutral atmospheric radio occultation (RO) soundings, and 1.6 million ionospheric RO soundings, serving more than 900 users from 50 countries. At the time of writing, COSMIC is producing approximately 2,500 GPS RO soundings per day, uniformly distributed around the globe. Several global operational centers, including ECMWF, NCEP, UKMO, Météo France, and Meteorological Service of Canada (MSC), are assimilating COSMIC data for global weather prediction, and all have demonstrated significant positive impacts. In this paper, we will present the status of the COSMIC mission, and discuss some recent scientific results from COSMIC. In particular, we show how COSMIC corrects the dry bias in global analyses and improved the prediction of the genesis of Hurricane Ernesto (2006). We examine the impact of COSMIC data on the analysis and prediction of an atmospheric river event that took place over the West Coast of the U.S. in November 2006. We present an analysis of atmospheric boundary layer height as estimated by COSMIC soundings, and their temporal and spatial variations. Finally, we describe the conceptual design for a possible COSMIC-II mission, which is being planned to succeed the COSMIC mission.

1. Introduction

Since the launch of the six-satellite constellation in April 2006, COSMIC has provided Global Positioning System (GPS) radio occultation (RO) data to support research and operation. All six satellites are operating, and providing data. As of October 2008, COSMIC had provided over 1.4 million neutral atmospheric sounding profiles, and over 1.6 million ionospheric profiles. Figure 1a shows the numbers of neutral atmospheric profiles generated per day throughout the mission. On average, COSMIC produces from 1,500 to 2,000 GPS RO soundings. Based on statistics provided by the UK Met Office, 90% of COSMIC data have latency shorter than 3 hours (Fig. 1b), from observation to operational use. Major global weather prediction centers, including ECMWF, NCEP, UK Met Office, Météo France, and MSC, are using this data for their operations (Cucurull and Derber 2008; Healy, 2008; Poli et al. 2008). All have reported significant positive impacts. COSMIC is now supporting more than 900 registered users from 50 countries. In collaboration with UNIDATA (http://www.unidata.ucar.edu/), COSMIC soundings are provided in a real-time data stream to support the university community. The scientific results from the first year of COSMIC operations are reported in Anthes et al. (2008). Additional significant results have been reported since.

In this paper, we will present a few selected studies conducted at UCAR on the scientific applications of COSMIC data. Section 2 presents results on the impact of COSMIC on the analysis of the genesis of Hurricane Ernesto (2006). Section 3 discusses the impact of COSMIC data on the analysis and prediction of an atmospheric river event that took place over the West Coast of the U.S. in November 2006. Results of the analysis of atmospheric boundary layer (ABL) heights are presented in Section 4. Finally, we present the conceptual design of a possible COSMIC-II mission in Section 5.

a)

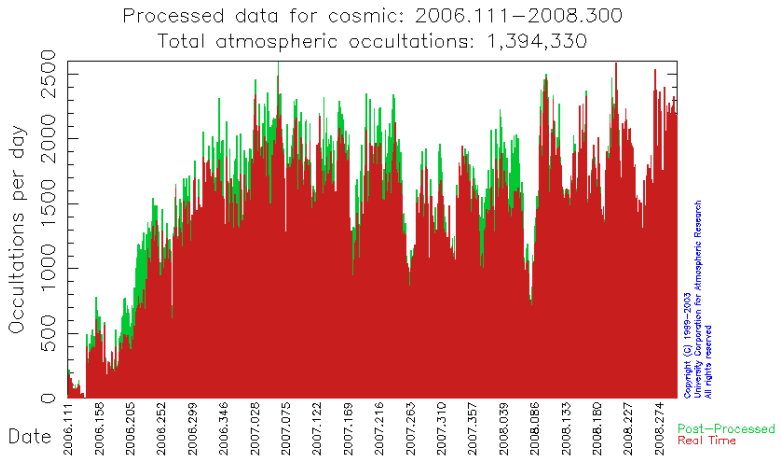

b)

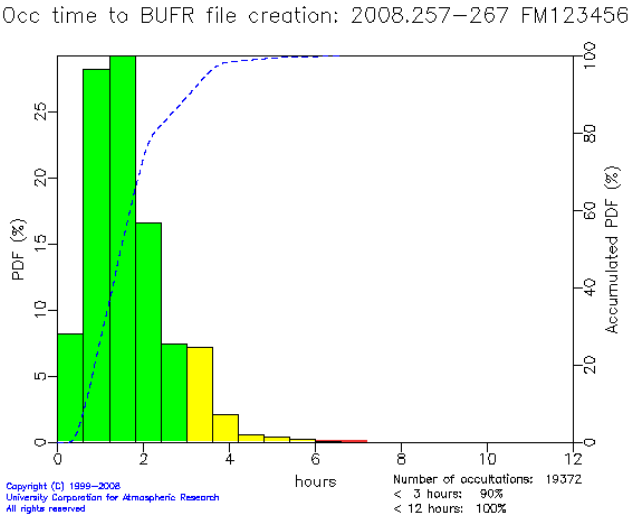

Figure 1(a) Daily COSMIC profile count throughout the mission. The red color shows the soundings from real-time processing. The green color shows the soundings from post-processing, which often is able to generate more sounding profiles. (b) The end-to-end data latency for COSMIC soundings based on operations at UKMO.

2. Impact of COSMIC on the analysis of Hurricane Ernesto in its genesis stage

Hurricane Ernesto (2006) was the first Atlantic hurricane to occur after COSMIC RO data became available, and major operational forecasts of the hurricane were unusually diverse. Ernesto formed as a tropical depression of 1007 hPa with maximum wind of 30 knots over the western Atlantic Ocean (62.4ºW, 12.9ºN) at 2100 UTC 24 August 2006. It then moved northwestward and reached tropical storm strength with minimum surface pressure of 1004 hPa and maximum wind of 35 knots at 2100 UTC 25 August. It continued to intensify as a tropical storm by 1200 UTC 26 August with a minimum surface pressure of 997 hPa. Later, Ernesto became a Category 1 hurricane with minimum surface pressure of 997 hPa and maximum surface wind of 65 knots at 1200 UTC 27 August. The hurricane dissipated on 1 September.

During the genesis period (21–25 August 2006) there were 171 COSMIC RO refractivity profiles within the tropical Atlantic Ocean study domain (not shown); 56 of these soundings were located within 1500 km of Ernesto. Of these 56 soundings, 75% reached between 0 and 2 km above the surface. These data provide valuable information about synoptic-scale distribution of water vapor in the middle and lower troposphere in the vicinity of Ernesto.

Liu et al. (2008) have conducted data assimilation experiments to assess the potential impact of COSMIC on the analysis of the genesis of Hurricane Ernesto. They use the WRF/DART ensemble data assimilation system to generate analyses by assimilating the RO refractivity profiles and satellite cloud winds during the period from August 16 to 25, which covers the genesis period of Ernesto. The observations are binned and assimilated every 6 hours, at 00UTC, 06UTC, 12UTC, and 18UTC each day. The WRF model is configured with a 36-km horizontal resolution with 35 vertical levels from the surface to 50 hPa (~20 km). The model domain covers the tropical Atlantic Ocean (0ºN-30ºN, 30ºW–100ºW). Thirty-six ensemble members are used in the assimilation. The initial (00 UTC August 16, 2006) and boundary ensemble mean conditions for the assimilation are obtained from the 1^{o}x1^{o} degree GFS (Global Forecast System) analysis produced by NOAA's National Centers for Environmental Prediction (NCEP). The initial and boundary conditions ensembles are generated by adding random draws from a distribution with the forecast error covariance statistics of the WRF 3D-Var data assimilation system to the mean fields.

To demonstrate the role of the RO data in the analysis, a companion analysis is also produced, assimilating only the cloud drift winds with no RO refractivity observations. There were also approximately 100 dropsonde profiles available in the vicinity of Ernesto during the period of the study. These dropsonde observations are withheld from the assimilation and are used to validate the resulting analyses.

Figure 2 shows the bias (time mean of analysis–observation) and RMS error of the specific humidity of the analyses verified against the dropsonde observations. The observations are binned into 7 bands in the vertical (300, 400, 500, 700, 850, and 1000 hPa) and then averaged over the horizontal domain and over all observations from the genesis period of Ernesto (21–25, August 2006). The water vapor analysis without the assimilation of RO observations has a large dry bias in the middle and lower troposphere. The mean error is as high as 0.6 g kg^{-1} at 850 hPa and 0.3 g kg^{-1} at 700 hPa. This dry bias reduces the moisture supply in the middle and lower troposphere, which is likely to hamper the analysis and prediction of the genesis of the tropical cyclone. With the assimilation of RO data, the dry bias is reduced, which should improve the analysis and prediction of the genesis of Ernesto.

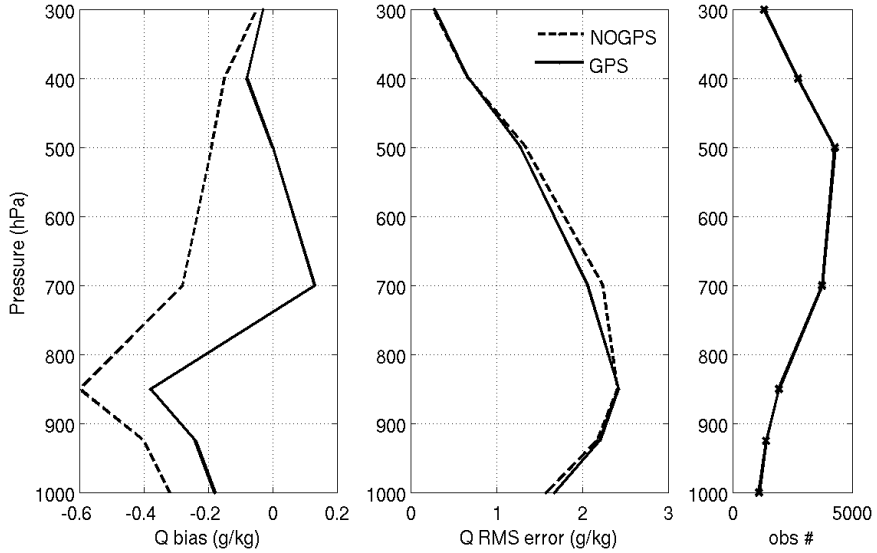

Figure 2 Vertical distribution of bias (analysis–observation, left panel) and RMS error (middle panel) for the specific humidity analysis verified against the dropsondes for the analyses with (solid line) and without (dashed line) the assimilation of the RO data averaged for the genesis period of Ernesto (21–25, August 2006); units g/kg. The right panel shows the total number of verifying dropsonde observations at each level. These are averaged over the entire domain in the horizontal. (From Liu et al. 2008)

The RO observations only slightly reduce the RMS error of the water vapor analysis in the middle troposphere, and the impact in the lower troposphere is marginal. A possible reason for this is that the dropsonde observations of water vapor may contain small-scale, high-frequency variations that cannot be resolved by the 36-km analyses. Another reason could be the fact that the assimilation is done in 6-hour windows centered at 00, 06, 12, and 18 UTC. The forward operators for the observations are not interpolated to the time of the dropsondes, which may introduce errors. Shorter assimilation windows of 3 hours or 1 hour would reduce this type of error.

Figure 3 shows sea-level pressure (SLP) analyses with and without the assimilation of RO data at 1200 UTC from August 21 to 25. At 1200 UTC 21 August, a weak low with a minimum pressure of ~1015 hPa appears near the eastern boundary around 12ºN, 42ºW in both cases. The system continues to develop over the next several days. At 1200 UTC 23 August, the analysis with the assimilation of RO data has developed a closed low of 1009 hPa near 58.6ºW, 12.8ºN. The analysis without the use of RO data has no indication of a closed depression, only a trough. At 1200 UTC 25 August, the RO analysis has a stronger depression of 1006 hPa near 65ºW, 14.3ºN, which is quite close to the observed low with similar intensity (1005 hPa observed). The analysis without RO data has a weaker depression with a minimum pressure of 1010 hPa and no evident closed circulation.

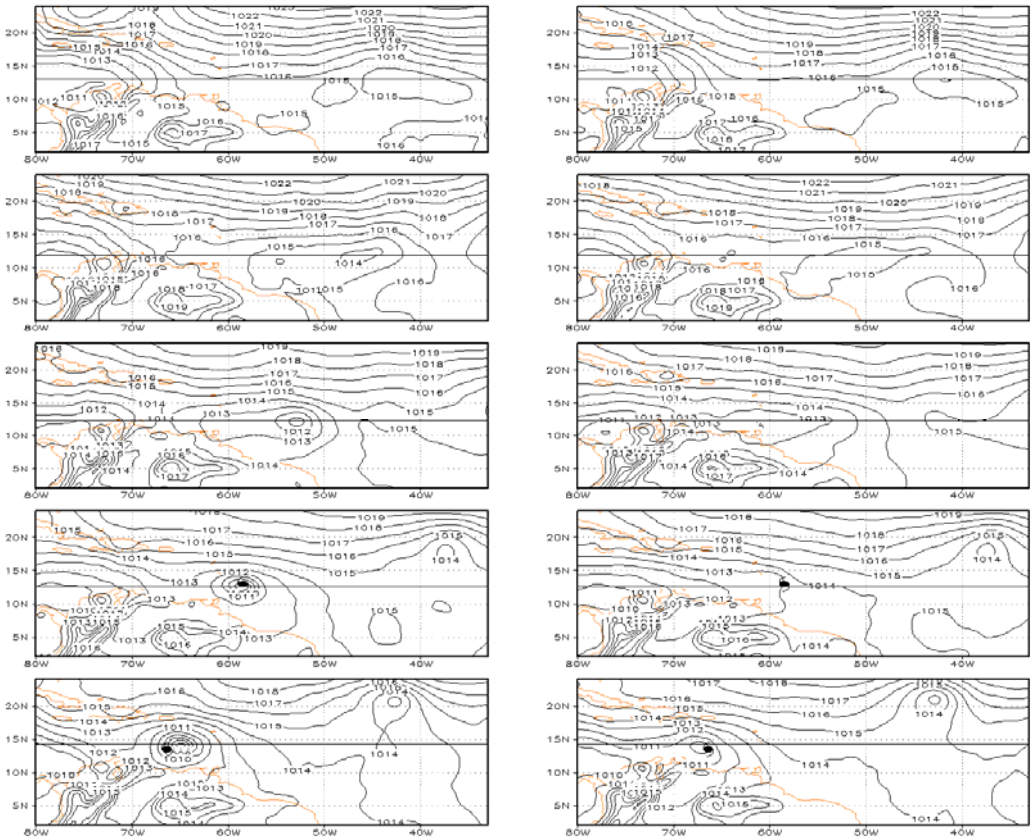

Figure 3 Sea-level pressure (SLP) analyses with (left) and without (right) RO refractivity data on 12 UTC August 21, 22, 23, 24, and 25, 2006 (from top to bottom). The hurricane symbol indicates the best track position for Ernesto. The solid line indicates the vertical cross sections cutting through the surface lows. Units: hPa. (From Liu et al. 2008)

Examining the analysis increments, which are mainly induced by the assimilation of RO data, can be used to assess the contributions of RO data to the analysis of water vapor. Figure 4 shows the vertical cross sections of the analysis increments for water vapor, averaged over the latitude belt of 9ºN-14ºN and for the 12-hour period centered at 1200 UTC of each day, from August 21 to 25, 2006. The RO data add significant amounts

of water vapor in the middle and lower troposphere in the vicinity of Ernesto, especially in the later part of the period. On August 21 and 22, the assimilation of RO data increases the water vapor by approximately 0.1 g/kg at the lower troposphere near the surface low. On August 23, the RO data assimilation adds much more water vapor with a maximum of about 0.3 g/kg at 900hPa in the lower troposphere near the low center. On August 24 and 25, the maxima of water vapor analysis increments are 0.3 and 0.5 g/kg at 800 hPa and 700 hPa, respectively, in the vicinity of the developing low. The increments of water vapor analysis have a horizontal scale of a few thousand kilometers. This is consistent with the results from Fig. 2, which shows that the RO data reduce the dry bias of the analysis.

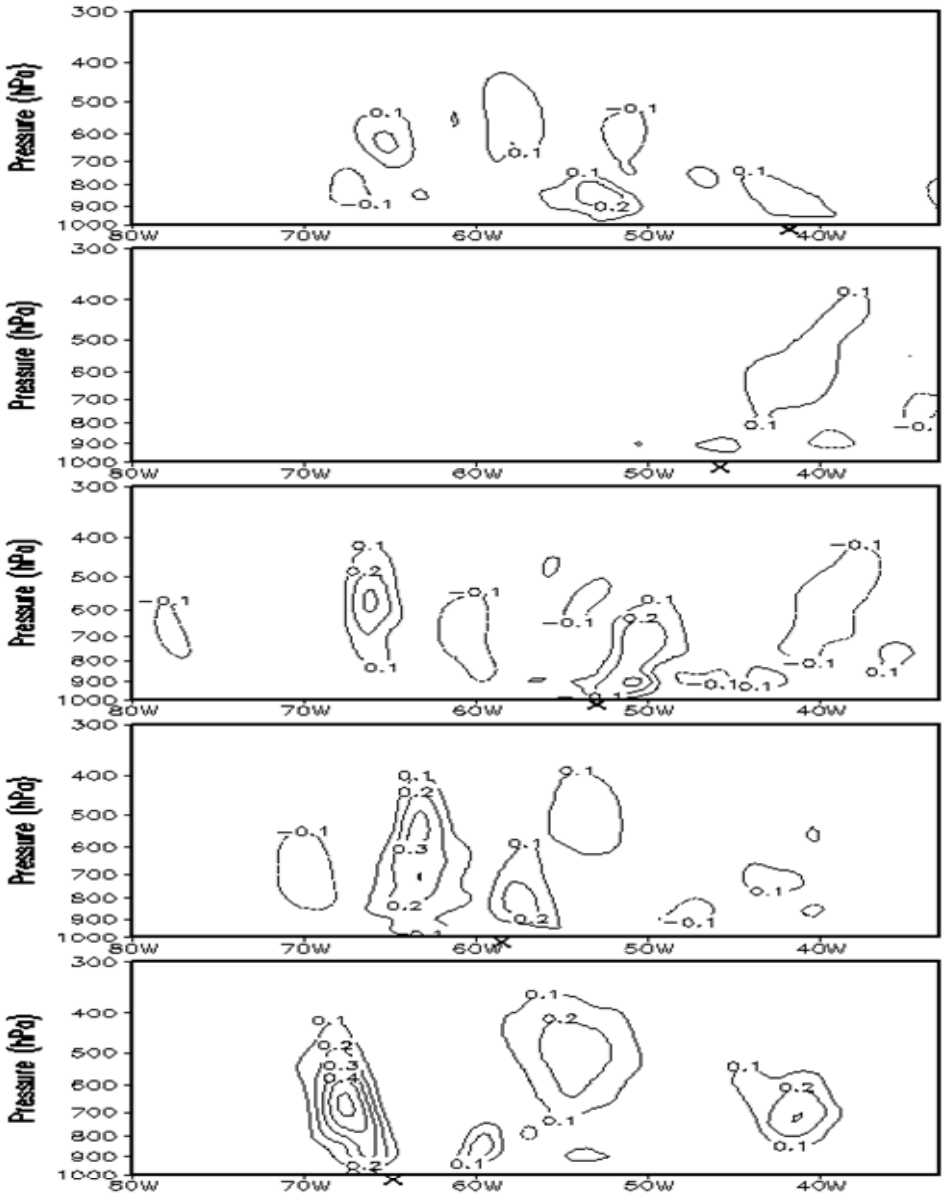

Figure 4 Vertical–longitudinal cross sections of the analysis increments for water vapor averaged for the latitudes of 9ºN-14ºN for analyses with RO refractivity observations. Increments are averaged for a 12-hour period centered at 12 UTC of each day from August 21 to 25, 2006 (from top to bottom). The symbol "x" indicates the longitude of the incipient lows in the analysis. Units: g/kg. (From Liu et al. 2008)

These results suggest that the assimilation of RO refractivity observations can reduce the dry bias of the water vapor analysis in the middle and lower troposphere. As a result, a better analysis of the genesis of Ernesto is produced.

3. Impact of COSMIC on the analysis and prediction of an atmospheric river event

An *atmospheric rive*r (AR) is a narrow band of strong horizontal water vapor flux associated with polar cold fronts. The AR over the eastern North Pacific Ocean often brings a significant amount of water vapor, causing extreme precipitation and flooding events over the West Coast of the United States. The AR plays a significant role in transporting moisture from the tropical reservoir to the middle latitudes. These systems often take place over the east Pacific Ocean, based on a record of the past ten years. Many studies have shown that ARs are critical contributors to extreme precipitation and flooding events of the West Coast of the U.S. (Ralph et al. 2004; Neiman et al. 2008).

An intense AR developed over the eastern North Pacific Ocean in early November 2006. Neiman et al. (2008) conducted a detailed analysis of this event, using available satellite (including GPS RO data from COSMIC) and other traditional observations. The November 6–7 2006 AR event was ranked by Neiman et al. (2008) as the first- or second-most intense storm among the 119 cases that occurred over the past nine years. Numerous locations in northwest Oregon and southwest Washington reported more than 7 inches of precipitation in a single day (most of them on November 6). Lees Camp in the Oregon Coast Range, a NOAA hourly rainfall station, recorded 14.3 inches of precipitation on the 6th, which broke Oregon's 24-hour rainfall record.

Ma et al. (2008) studied the impact of GPS RO data on the analysis and prediction of this AR event using the NCEP regional GSI data assimilation system, together with the NCAR Advanced Research WRF (ARW) model (Skamarock et al. 2005). The model physics for both ARW 36-km and 12-km grids are the same, and include the Rapid Radiative Transfer Model (RRTM) long wave radiation, the Dudhia shortwave radiation scheme, the YSU PBL scheme, the Kain-Fritsch (new Eta) cumulus parameterization, and the new Thompson graupel microphysics parameterization. The grid's dimensions are 135x118 and 160x160 in east-west and north-south directions in the 36-km and 12-km domains, respectively. The assimilation was performed only on the coarse domain with 36-km resolution. The assimilation was performed using both the local refractivity operator (Cucurull et al. 2007) and the non-local excess phase observation operator (Sokolovskiy et al. 2005). The model has 38 vertical levels with the top of the model located at 50 hPa.

To assess fully the impact of GPS RO soundings on this intense atmospheric river event, two sets of experiments are conducted: First, we perform a cycling assimilation experiment from 0000 UTC 3 November to 1800 UTC 9 November 2006, in which GSI is used for the analysis component and the ARW model is used for the 6-h forecast component; second, a 24-h forecast impact experiment from 1200 UTC 6 which is carried out with the ARW model. The experiment design is illustrated in Fig. 5.

Three experiments have been performed in each set:

1. The "CTRL" experiment that assimilates the same conventional and satellite measurements used in the NCEP operations.
2. The "LOC" experiment, which is identical to the CTRL, except that GPS RO refractivity profiles are assimilated with the local refractivity observation operator.
3. The "NON-LOC" experiment, which is identical to the CTRL, except that GPS RO refractivity profiles are assimilated with the non-local excess phase observation operator (Sokolovskiy et al. 2005).

Here we present the analysis at 0600 UTC 7 November 2006 to illustrate the influence of GPS RO profiles on the analysis of this event. This selected analysis is extracted from the week-long cycling assimilation experiment starting from 0000 UTC 3 November 2006 (Fig. 5). Figure 6 shows the precipitable water vapor

(PWV) at 0600 UTC 7 November 2006 derived from the analysis with NON-LOC experiment. The figure clearly shows the concentration of precipitable water along the narrow band of atmospheric river. The band of atmospheric river shown in the PWV analysis compares favorably to that of the SSM/I satellite infrared water vapor (IWV) image, shown in Fig. 2a of Neiman et al. (2008). This similarity is reflected in both the strength and range of PWV values associated with the atmosphere river.

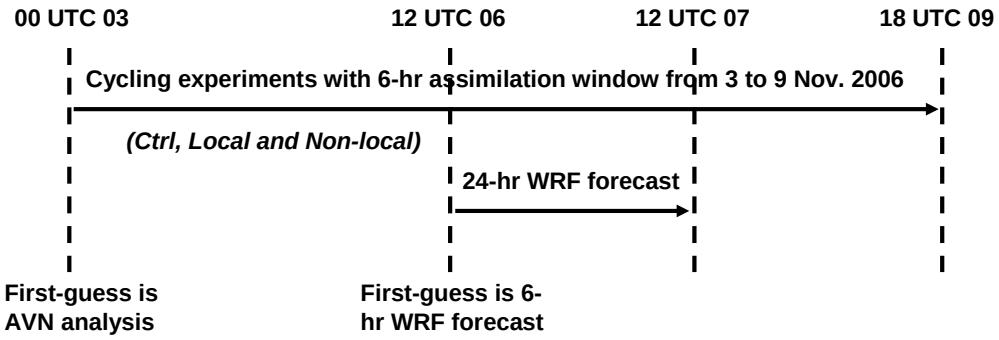

Figure 5 Experimental design of assimilation cycling for one week (0000 UTC 03 ~ 1800 UTC 09 November 2006) and 24-h forecast from 1200 UTC 06 November 2006. (From Ma et al. 2008)

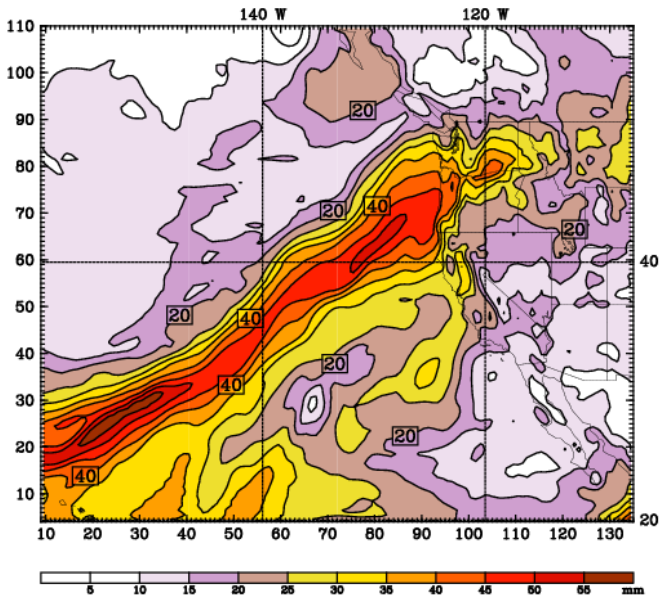

Figure 6 Analysis of PWV in the cycling assimilation experiment when GPS RO soundings are assimilated with Non-local operator, valid at 0600 UTC 07 November 2006. (From Ma et al. 2008)

The difference field in PWV between CTRL and LOC is presented Fig. 7a, and the difference between CTRL and NON-LOC in Fig. 7b. These two difference fields are both valid at 0600 UTC 7 November 2006. They show that the impact of GPS RO data assimilation on this event occurs primarily in the vicinity of the atmospheric river, irrespective of the use of the local or non-local operator to assimilate the GPS RO soundings. It is important to note that the distribution of GPS RO soundings is relatively uniform over the assimilation domain in the cycling experiments (not shown). Another noticeable result is that the NON-LOC experiment produces larger changes (both in the amount and area) than LOC (comparing Fig. 7a with Fig. 7b**)**. As will be shown later, these differences in the moisture analysis will have an influence on precipitation prediction.

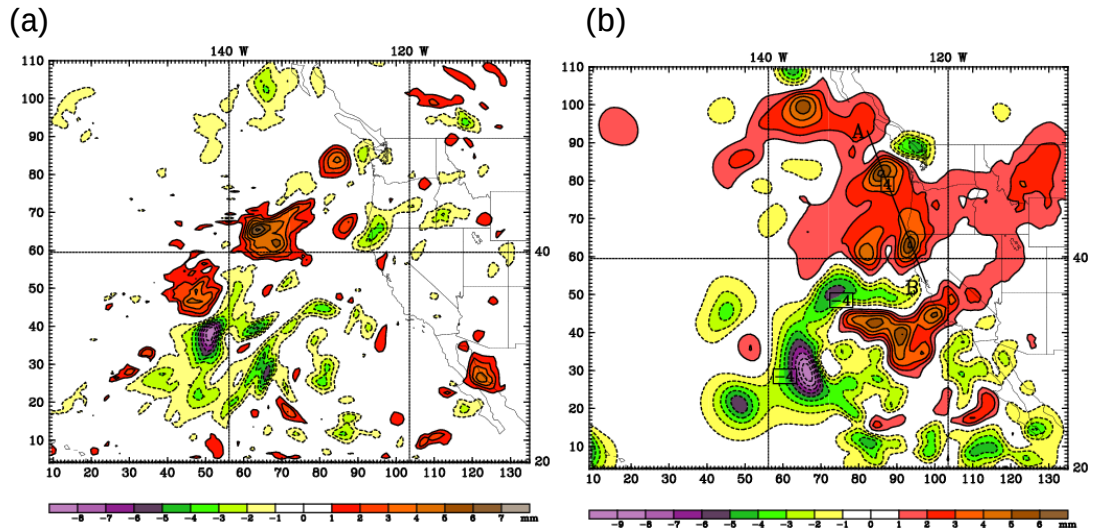

Figure 7 PWV differences in the cycling assimilation experiment between: (a) LOC and CTRL experiments; and (b) NON-LOC and CTRL experiments valid at 0600 UTC 07 November 2006. (From Ma et al. 2008)

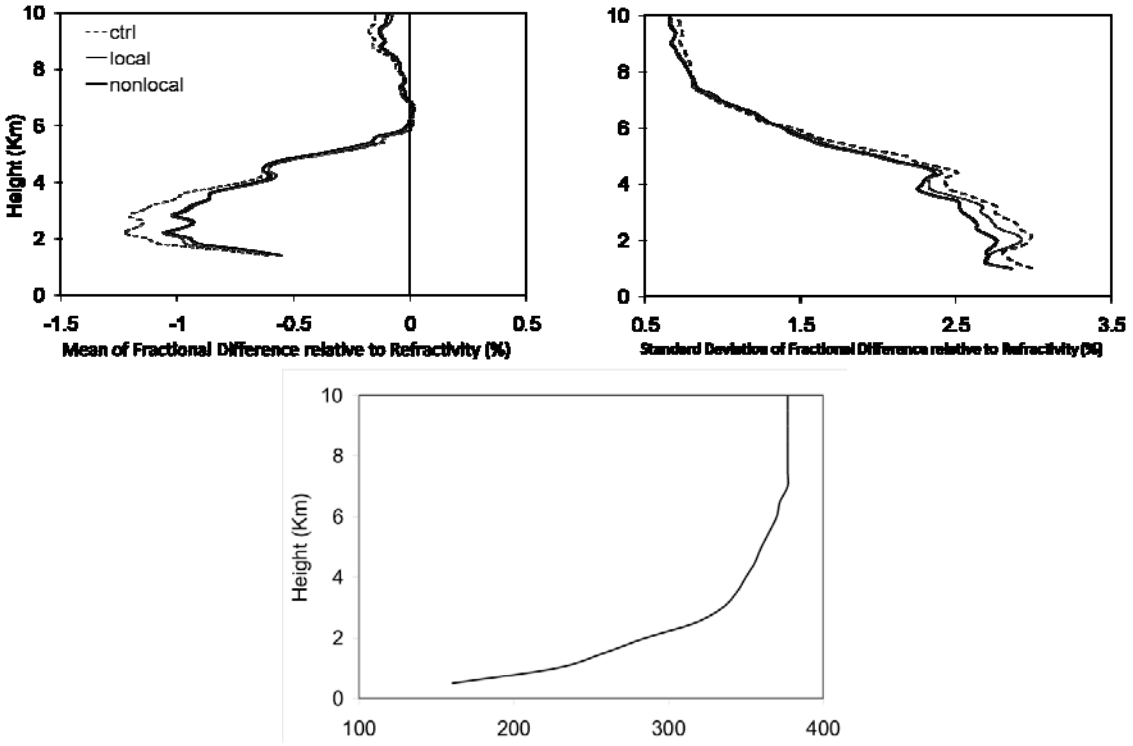

Figure 8 The statistics of fractional difference for the assimilation domain from 0000 UTC 03 to 1800 UTC 09 November 2006. Mean (left panel) and Standard Deviation (middle panel) errors of 6-h WRF forecasts verified against GPS RO refractivity for CTRL (dashed curve), LOC (thin curve) and NON-LOC (thick curve). The right panel shows the total number of GPS soundings used for verification at each level during the one-week cycling period. (From Ma et al. 2008)

To gain insights into the impact of GPS RO data assimilation, we show in Fig. 8 the vertical profiles of the mean and standard deviation errors of 6-h WRF forecasts (which serve as the "background" for the data assimilation) verified against GPS RO refractivity observations. It is clear that both the mean and standard deviation errors of LOC and NON-LOC with GPS RO data are smaller than the CTRL errors at all model levels, but especially at the lower level (below 5km). The fact that 6-h forecasts based on analyses with the assimilation of GPS RO data verified better with the observations indicates that these analysis are improved

with the assimilation of the GPS RO data (with either local or non-local observation operators). For example, the GPS RO measurements reduce a negative bias in the layer between 2 to 5 km from ~ -1.2% (for CTRL) to -1.0% for LOC and NON-LOC. A closer look shows that NON-LOC provides a superior performance (i.e. a more accurate 6-h forecast), particularly in terms of standard deviation error, when compared to the LOC experiment. Again, this suggests that the use of non-local excess phase observation operators can assimilate the GPS RO data more effectively for this atmospheric river event with significant horizontal gradients.

During this atmospheric river event, heavy rainfall took place across the Pacific Northwest of the U.S., mainly in the states of Washington and Oregon, on 6~8 November 2006. To further evaluate the GPS RO observation impact on this forecast event, we performed a 24-h forecast with 12-km higher resolution starting at 1200 UTC 6 (Fig. 5). The 24-h observed precipitation was shown in Fig.9a, ending at 1200 UTC 7 November. Three heavy rainfall centers are located in Washington and Oregon. The CTRL experiment without GPS RO observation produces precipitation with a pattern similar to that of observed rainfall, but with weaker intensity than that observed. Comparing with the forecast from CTRL (Fig. 9b), LOC (Fig. 9c) and NON-LOC (Fig. 9d), all produce larger rainfall amounts, illustrating the positive impact of GPS RO data assimilation. The rainfall amount from NON-LOC is the largest, and compares most favorably with the observed precipitation, again illustrating the superior performance of the non-local excess phase observation operator.

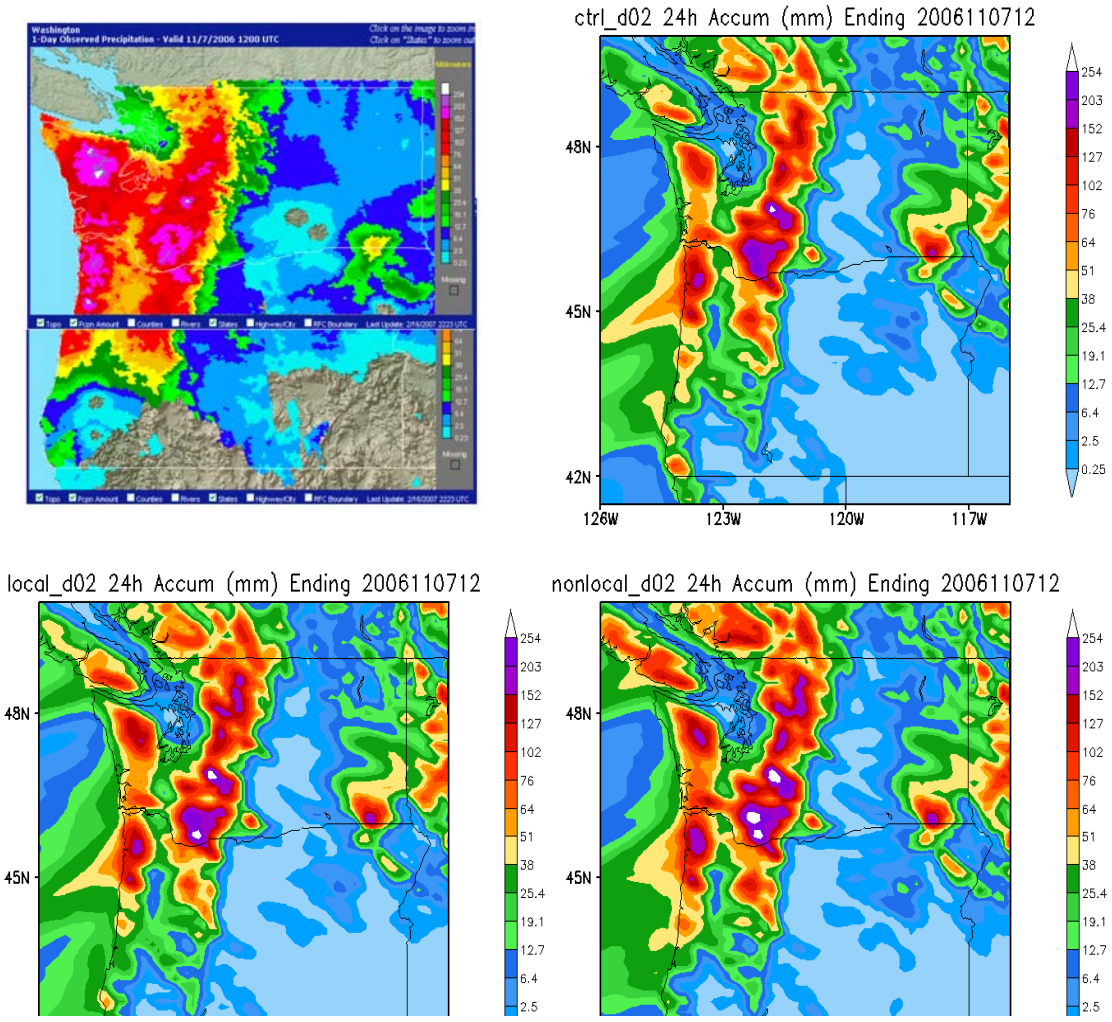

Figure 9 The 24-h precipitation ending at 1200 UTC 7 November 2006 is mainly over the Washington and Oregon states. Panel at upper left is based on gauge observations, and panels at upper right, lower left and lower right are from CTRL, LOC and NON-LOC experiments, respectively. (From Ma et al. 2008)

4. Atmospheric boundary study with COSMIC GPS RO data

With the use of an "open-loop" tracking technique (Sokolovskiy 2001), COSMIC GPS RO soundings can penetrate well into the atmospheric boundary layer. In line with pre-launch expectations, the statistics since launch indicate that more than 70% of COSMIC soundings penetrate below 1 km over the tropics, and more than 90% over high latitudes (Anthes et al. 2008). In comparison, in earlier satellite missions (e.g., CHAMP), which use phase-locked-loop tracking, fewer than 10% of soundings penetrate below 1 km over the tropics. Thus, COSMIC provides a novel opportunity to use GPS RO soundings to study the atmospheric boundary layer (ABL) and its variations. Typically, the top of ABL is accompanied by inversion layer, which is reliably detected in RO via large lapse of the bending angle or refractivity gradient (Sokolovskiy et al. 2006). Both methods yield similar results.

Figure 10 compares the ABL heights estimated from COSMIC GPS RO over North America between summer of 2007 (top panel) and winter of 2006/2007 (bottom panel). The ABL height is estimated based on the bending angle lapse rate. This shows a lower ABL height off the coast of California in the summer, compared with that over the eastern two thirds of North America. In the winter, the situation is reversed, with shallower ABL height over land than that over the oceans (e.g., California coastal waters, and Gulf of Mexico).

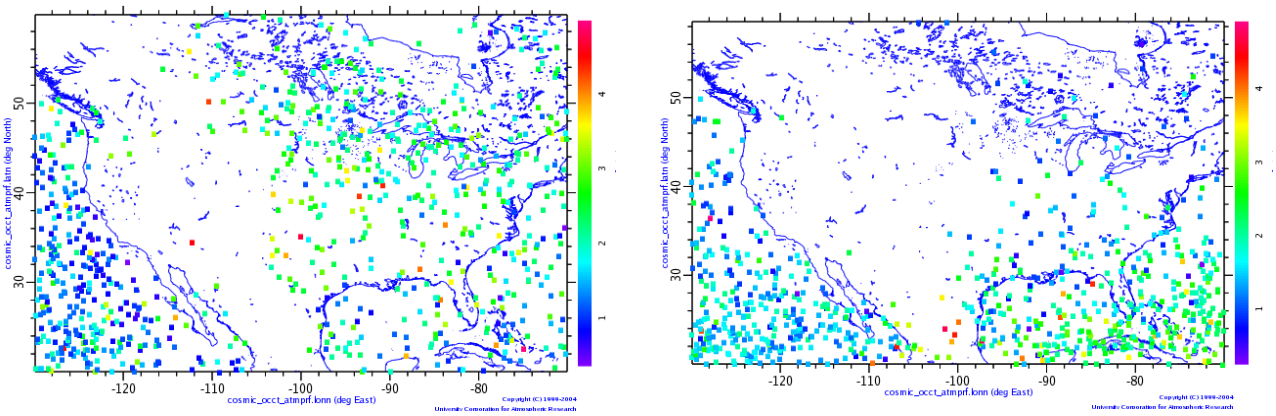

Figure 10 The atmospheric boundary layer height as estimated by COSMIC GPS RO soundings during the summer (top) and winter (bottom). The height of ABL is color-coded following the color scale on the right. Top panel is for the summer months (Jun–Aug 2007) and bottom panel is for the winter months (Dec 2006–Feb 2007).

Figure 11 shows the ABL height as detected by COSMIC GPS RO refractivity profiles over a one-year period, stratified into four different seasons. For this analysis, the ABL height is estimated based on the break point of the refractivity profile. The figure illustrates very interesting spatial variability of ABL height over the oceans. For example, we see the low ABL height off the California coast in the spring. Similarly, the ABL height is very low off the coast of South America, at about 20ºS in the summer and fall. The ABL height increases considerably westward from the West Coast of South America, reaching a maximum at around 140ºW. The figure also shows significant seasonal variations over many places around the globe. For example, over the western North Pacific, the ABL height reaches a minimum in the summer, and a maximum in the winter. When interpreting maps in Fig.11, we note that the used method does not give reliable estimation of the ABL height in the regions where strong inversions are rarely observed, e.g., in the high latitudes and in the intertropical convergence zone (ITCZ).

The ABL height as estimated by COSMIC GPS RO soundings can be used to compare to global analyses. Figure 12 shows the difference in ABL height between COSMIC and ECMWF global analyses. For this comparison, we interpolate the ECMWF global analysis to the GPS RO sounding positions, and perform the

ABL height analysis using exactly the same algorithm used to analyze the COSMIC observations. In general, we find that the COSMIC ABL heights are higher than those from the ECMWF analysis. The differences are, in general, within a few hundred meters. Larger differences (exceeding 500 m) can be found over the tropics at some places. However, over the southern oceans, ECMWF often shows higher ABL heights. At this point, one cannot say for sure which is more accurate. It would be interesting to perform additional verification studies using independent data sets from special field programs, such as VOCALS (http://www.eol.ucar.edu/projects/vocals/).

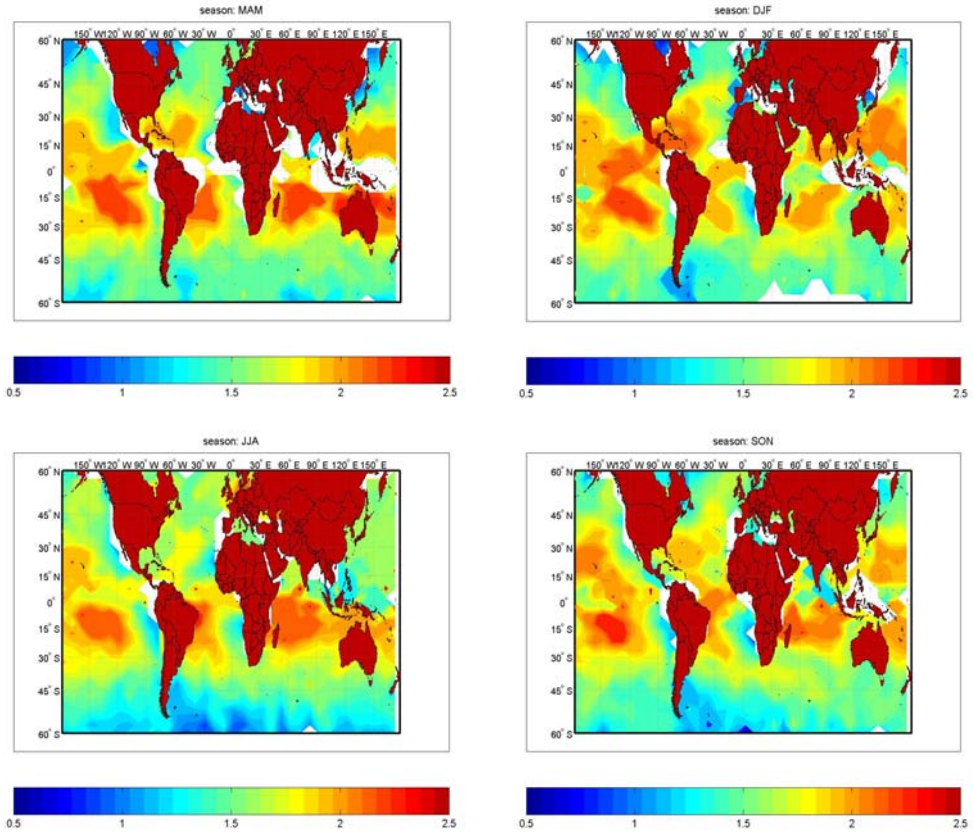

Figure 11 The ABL height estimated by COSMIC over a one-year period, from September 2006 through August 2007. (Upper left: March–May. Upper right: Dec–Feb. Lower left: Jun–Aug. Lower right: Sep–Nov. Color scale gives height in km.)

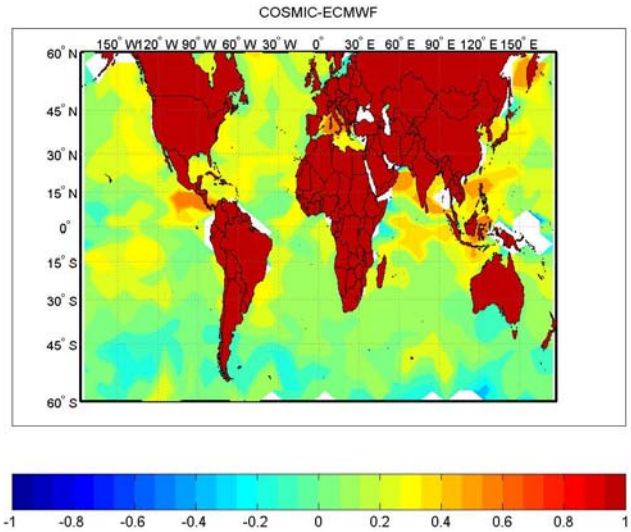

Figure 12 ABL height differences between COSMIC and ECMWF global analysis, averaged over a one-year period. Color code gives difference in km.

5. The conceptual design of COSMIC-II

With the continued provision of high-quality GPS RO data, COSMIC is demonstrating the significant value of radio occultation observations to atmospheric sciences, both in terms of research and operations. COSMIC is a science mission, designed to demonstrate the usefulness of GPS RO data in operational numerical weather prediction, climate monitoring, and space weather forecasting. It is not an operational mission (as defined by NOAA), with all the redundancy and robustness. The nominal life for the COSMIC satellites is approximately five years (2006-2011). A gradual degradation of the COSMIC constellation can be expected in 2011. With the demonstrated positive impact of RO data in weather prediction, climate and ionospheric research, it is highly desirable to begin serious planning for a follow-on constellation. In fact, the World Meteorological Organization (WMO, 2007) and the U.S. National Research Council (NRC, 2007) have both recommended continuation of RO observations operationally.

Following a FORMOSAT-3/COSMIC Workshop in Taiwan in October 2008, NOAA and NSPO are considering a possible COSMIC-II mission. It is anticipated that this COSMIC-II mission will make use of the next generation of JPL RO receivers, which can track radio signals from three GNSS systems, including GPS, GALILEO, and GLONASS. Efforts will also be made to expedite the data downlink, allowing significant reduction of data latency. This will allow the COSMIC-II data to be even more useful for both weather and space weather forecasting. Improved antenna design will be considered to increase the antenna gain, resulting in higher-quality RO soundings. As of November 2008, the plans are not yet firm, but the target COSMIC-II system is expected to consist of at least 12 low-Earth-orbiting (LEO) satellites, producing ~15,000 GPS RO soundings per day. Figure 13 gives an illustration of the density of RO soundings in the continental U.S., with 12 LEOs tracking only GPS, GPS + GLONASS, and GPS + GLONASS + GALILEO. The data density varies from 3.1, 5.9 to 9.1 over a 500 km x 500 km domain over a 24-h period. Based on the results from COSMIC, with a sizeable increase in higher-quality soundings, there is little doubt that COSMIC-II will be a quantum jump forward from the current COSMIC mission.

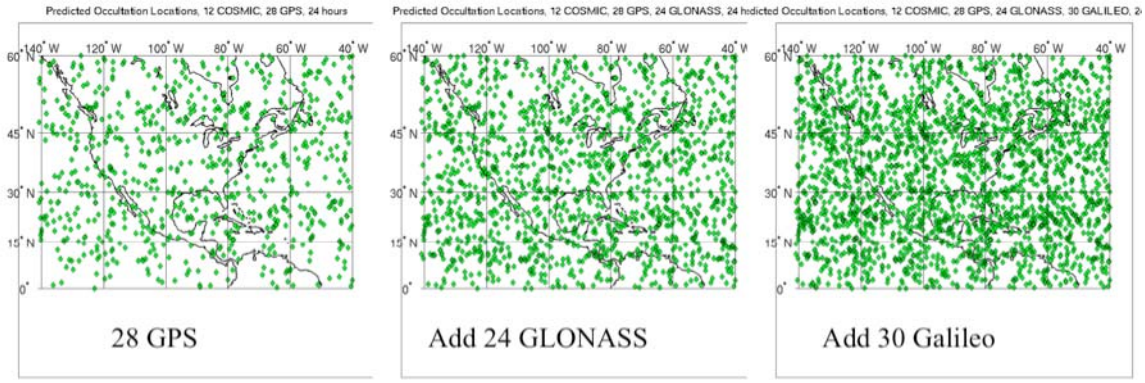

Figure 13 Distribution of RO soundings for a 12-satellite constellation, tracking 28 GPS (left panel); plus 24 GLONASS (middle panel); and add another 30 GALILEO satellites (right panel).

Acknowledgement

We would like to thank Jeff Anderson, Doug Hunt, Paul Neiman, Marty Ralph, Chris Rocken, and Bill Schreiner for their contributions to the work presented here and Sara Frank Bristow for her technical editing. This work is supported by the NCAR ASP Graduate Visitor Program, NCAR/MMM, NCEP/EMC and JCSDA, and NSF under corporate agreements with UCAR awards #ATM-0410018 and INT-0129369, and the National Aeronautics and Space Administration under grant NNX08AI23G.

References:

Anthes, R. A., and co-authors, 2008: The COSMIC/FORMOSAT-3 Mission: Early Results, *Bull. Amer. Met. Soc.*, **89**, 313-333.

Cucurull, L., L. C. Derber, R. Treadon, and R. J. Purser, 2007: Assimilation of Global Positioning System radio occultation observations into NCEP's Global Data Assimilation System, *Mon. Wea. Rev.,* **135**, 3174-3193.

Cucurull, L., and J. C. Derber, 2008: Operational implementation of COSMIC observations into the NCEP's global data assimilation system. Wea. Forecasting, (in press).

Healy, S. B., 2008: Forecast impact experiment with a constellation of GPS radio occultation receivers. *Atmos. Sci. Let*. Doi: 10.1002/asl.169.

Liu H., J. Anderson, Y. Chen, and Y.-H. Kuo, 2008: Exploring potential benefits of radio occultation observations to the analysis of water vapor and tropical cyclone genesis. Mon. Wea. Rev., (submitted).

Ma, Z., Y.-H. Kuo, B. Wang, W.-S. Wu, S. Sokolovskiy, P. J. Neiman, and F. M. Ralph, 2008: Assimilation of GPS radio occultation data for an intense atmospheric river with the NCEP regional GSI system. Mon. Wea. Rev. (submitted).

Neiman, P., F. M. Ralph, G. A. Wick, Y.-H. Kuo, T.-K. Wee, Z. Ma, G. H. Taylor, and M. D. Dettinger, 2008: Diagnosis of an intense atmospheric river impacting the Pacific Northwest: Storm summary and offshore vertical structure observed with CSOMIC satellite retrievals. *Mon. Wea. Rev.*, (in press).

NRC, 2007: Earth Science and Applications from Space-National Imperatives for the next Decade and Beyond. National Academies Press, Washington, D.C. 428 pp.

Poli, P., P. Moll, D. Puech, F. Rabier, and S. B. Healy, 2008: Quality control, error analysis, and impact assessment of FORMOSAT-3/COSMIC in numerical weather prediction. *Terrestrial, Atmospheric and Oceanic Sciences* (in press).

Ralph, F.M., P.J. Neiman, and G.A. Wick, 2004: Satellite and CALJET aircraft observations of atmospheric rivers over the eastern North-Pacific Ocean during the winter of 1997/98. *Mon. Wea. Rev.*, **132**, 1721-1745.

Skamarock, W. C., J. B. Klemp, J. Dudhia, D. O. Gill, D. M. Barker, W. Wang and J. G. Powers, 2005: A Description of the Advanced Research WRF Version 2. NCAR technical note NCAR/TN–468+STR, 100 pp.

Sokolovskiy, S., 2001: Tracking tropospheric radio occultation signals from low Earth orbit. *Radio Sci.*, **36**(3), 483-498.

Sokolovskiy, S., Y. H. Kuo, and W. Wang, 2005: Assessing the accuracy of linearized observation operator for assimilation of the Abel-retrieved refractivity: case simulation with high-resolution weather model. *Mon. Wea. Rev.*, **133**, 2200-2212.

Sokolovskiy S., Y.-H. Kuo, C. Rocken, W. S. Schreiner, D. Hunt, and R. A. Anthes, 2006: Monitoring the atmospheric boundary layer by GPS radio occultation signals recorded in the open-loop mode. *Geophys. Res. Lett.*, **33**, L12813, doi:10.1029/2006GL025955.

WMO, 2007: Workshop on the Re-design and Optimization of the Space-based Global Observing System-FINAL REPORT. WMO Headquarters, Geneva, 12 pp.